Root responses to different types of TiO2 nanoparticles and bulk counterpart in plant model system Vicia faba L.

(Article begins on next page)

05 November 2024

1   **Root responses to different types of TiO$_2$ nanoparticles and bulk counterpart in plant**

2   **model system *Vicia faba* L.**

3

4   Monica Ruffini Castiglione[1*], Lucia Giorgetti[2], Lorenza Bellani[2,3], Simonetta Muccifora[3], Stefania Bottega[1],

5   Carmelina Spanò[1]

6

7   [1]Department of Biology, University of Pisa, Via Ghini 13, 56126 Pisa, Italy; [2]Institute of Agricultural Biology

8   and Biotechnology, UOS Pisa, CNR, Via Moruzzi 1, 56124 Pisa, Italy; [3]Department of Life Sciences, University

9   of Siena, Via A. Moro 2, 53100 Siena, Italy

10
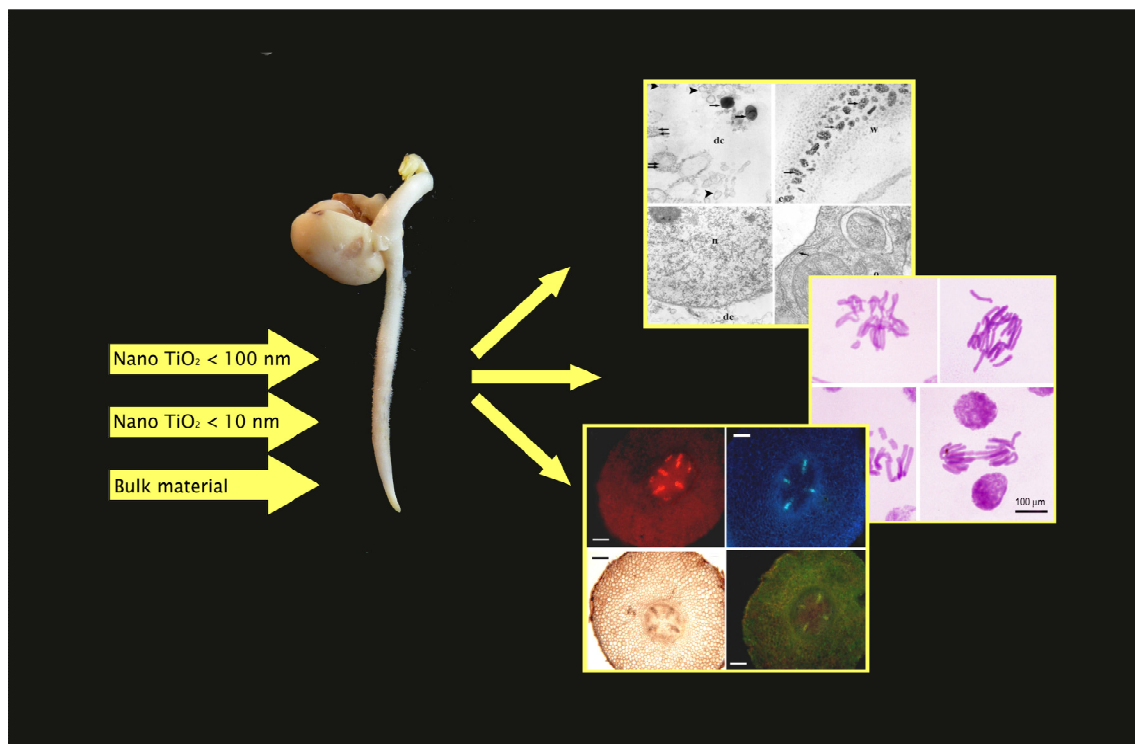
11

12   *Corresponding author: monica.ruffini.castiglione@unipi.it, tel. +390502211317

13   All the authors contributed equally to the article

14

Abstract

The aim of the present work was to study , in the model system *Vicia faba* L., the potential stress-induced response to a commercial source of TiO_2 nanoparticles (NPs) <100nm (tetragonal crystals), to a TiO_2-NPs laboratory-made sample <10nm (spherical shape), and to the corresponding bulk material, recently classified as possibly carcinogenic to humans.

The above materials were applied to *V. faba* seeds up to early seedling development; different endpoints were considered to estimate possible phytotoxic and genotoxic effects at ultrastructural, cyto-histological and physiological level. Oxidative stress and antioxidant response were evaluated by biochemical approach and *in situ* histochemical techniques. Ultrastructural studies demonstrated that the applied NPs were internalized in root plant cells but the most damages to the cellular appearance followed bulk material treatment. Our results on seed vigor index, on aberration index, on the evaluation of oxidative stress and of induced antioxidant response demonstrated that TiO_2-NPs may exert specific actions at different levels of toxicity, depending on their size and shape and that the bulk counterpart seems to provoke the major adverse effects in *V. faba* root.

1. Introduction

Nanotechnologies are a tremendous opportunity for their positive impact in many sectors of economy, in industrial applications and in scientific research, but with unavoidable environmental emission and release of new chemicals. Nanoparticles (NPs) find their way into aquatic, terrestrial and atmosphere environments, where their fate and behaviour depend on the particle type, on their aggregation tendency and on bioavailability (Hotze et al., 2010). Therefore plants, organisms that strongly interact with their immediate environment, are expected to be affected by their exposition to NPs. As a consequence NPs have been recently included among the emerging contaminants by USEPA (2010). From the first decade of two thousand the first papers published on the potential effects of NPs on higher plants (Ma et al., 2010; Navarro et al., 2008; Ruffini Castiglione and Cremonini, 2009) evidenced some crucial points:

a) NPs, strongly enhancing or modifying the properties of the bulk materials, can interact in a non-predictable way with the environment and the living organisms;

b) NPs can explicate their actions depending on both the chemical composition and on the size and/or shape of the particles themselves;

c) NPs effects depend on the plant organism considered and on the variety of endpoints employed, sometimes making difficult comparative studies. In addition, the evaluation of specific effects, although fundamental to the understanding of the toxicity mechanisms, cannot be extended to all plant systems.

In the light of these considerations we can emphasize that the studies conducted so far on the phytotoxicity of NPs have produced data inadequate to characterize unambiguously their actions on plants, although many results demonstrate effects on *in vitro* cell culture,

3

64 embryogenesis, growth, biochemical processes and gene expression (Giorgetti et al., 2011;

65 Kaveh et al., 2013; Poborilova et al., 2013).

66 TiO_2-NPs, for their high stability, anticorrosive properties, redox selectivity, low production

67 costs and their wide spectrum of new applications, are among the top five NPs used in

68 consumer products (Chuankrerkkul and Sangsuk, 2008). Most of NPs applications are related

69 to their characteristics of white pigment, four million tons being consumed annually

70 worldwide (Ortlieb, 2010). Furthermore TiO_2-NPs are widely used in common products

71 (toothpastes, sunscreens, cosmetics, food products), in specific fields of medicines and

72 pharmaceuticals, in certain sectors of agriculture and in environmental cleanup technologies

73 (Bhawana and Fulekar, 2012; Liu, 2011).

74   Previous studies evidenced both positive and negative effects of TiO_2-NPs on plants. Part

75 of the scientific literature reports their significant improvement of germination, of shoot and

76 root growth, of chlorophyll content, of transpiration and of water use efficiency (Raliya et al.,

77 2015; Seeger et al., 2009; Song et al., 2013; Zheng et al., 2005). On the contrary, other papers

78 report that plants can be harmed by TiO_2-NPs with decrease in biomass, delayed germination,

79 influence on mitotic index and genotoxic effects (Du et al., 2011; Ruffini Castiglione et al.,

80 2011), DNA fragmentation, reactive oxygen species (ROS) production (Ghosh et al., 2010;

81 Ruffini Castiglione et al., 2014) and changes in micro-RNA expression (Frazier et al., 2014).

82   The experimental design of this work was scheduled to study the potential effects of TiO_2-

83 NPs in the model system *Vicia faba*, at 72 h of seed germination, the most widely used

84 treatment time assessing chemical-induced acute adverse effects (Baderna et al., 2015).

85   We choosed a middle-low exposure concentration that possibly might reproduce an actual

86 environmental exposure, estimated by recent probabilistic material-flow modelling studies

87 (Praetorius et al., 2012). On the basis of previous data showing negative effects only induced

88 by high TiO_2 NPs concentrations (Ruffini Castiglione et al., 2014), we hypothesized plant

4

89 responses, not necessarily associated to toxic effects.

90 We employed two types of TiO$_2$-NPs to assess if different responses in function of

91 different particle size and characteristics were elicited. In addition, as corresponding bulk

92 material, considered for decades an inert and safe material has been recently classified as

93 possibly carcinogenic to humans (Group 2B carcinogen, IARC 2010), we tested also the

94 effects of the same concentration of this form. To evaluate the hypothesized effects of these

95 materials on *V. faba* seeds, we considered different cytological, physiological, histochemical

96 and biochemical endpoints. Given that NPs can influence plant growth and development

97 directly entering plant cells by means of different penetration mechanisms (Chichiriccò and

98 Poma, 2015) or even without being internalized, a further aim of our work was to understand

99 how these materials can affect *V. faba* root ultrastructure in function of the shape and of the

100 size of the NPs.

101

102 **2. Materials and methods**

103 *2.1. Seed germination and seedling development*

104 Seeds of *Vicia faba* L. var. *minor* were washed over night in tap water, germinated at 24±1

105 °C for 72 h in the dark in Petri dishes in water (control, sample C), in a suspension of two

106 rutile/anatase TiO$_2$-NPs: < 100 nm (sample S: tetragonal crystals, from Sigma-Aldrich, USA);

107 < 10 nm (sample P: spherical shape, produced by pulsed laser ablation in liquids) (Giorgetti et

108 al., 2014), kindly provided by PlasmaTech, Pisa (Italy) and in bulk TiO$_2$ (sample B, from

109 Sigma-Aldrich, USA). All the treatments were performed at the selected concentration of 50

110 mg/L. For all treatments 5 Petri dishes with 10 seeds each were set up. Three days after

111 treatment, the germination percentage and the seedling root length were evaluated in all

112 samples.

113 Vigour index (VI) was calculated with the following formula:

114   VI = Germination (%) x Seedling Growth (mm).

115   Roots were collected for cytological, histochemical and biochemical determinations as

116   described below.

117

118   *2.2. Transmission electron microscope (TEM)*

119   To evaluate morphology and size of the different TiO_2-NPs, a drop (10 µL, 50 mg/L) of

120   samples S and P was placed on TEM grids covered with formvar, allowed to settle and dry.

121   For TEM root observations, small cubes of control and treated roots were pre-fixed in

122   Karnovsky solution (Karnovsky, 1965), post-fixed in osmium tetroxide, dehydrated and

123   embedded in Epon 812-Araldite A/M mixture. Thin sections were stained with uranyl acetate

124   and lead citrate.

125   Isolated NPs and root sections were observed under a FEI Tecnai G2 Spirit electron

126   microscope at 100 kv.

127

128   *2.3. Cytological studies on root meristem*

129   Ten roots for each treatment were fixed in ethanol: glacial acetic acid (3:1 v/v) for 12 h.

130   Root tips were squashed and stained following Feulgen technique (Giorgetti and Ruffini

131   Castiglione, 2016).

132   At least 1000 nuclei, randomly selected for each slide, were analyzed by light microscope.

133   Perturbations in mitotic activity (mitotic index, MI, = number of mitosis/100 nuclei)

134   indicate cytotoxicity, while both micronuclei presence (MNC=Micronucleus frequency/1000

135   nuclei) and mitotic aberrations (aberration index, AI, = number of aberrations/100 nuclei)

136   indicate the genotoxicity of a treatment. The scored aberrations included chromosomal

137   bridges, fragments, lagging chromosomes, stickiness, aberrant metaphases and disturbed

138   anaphases in dividing cells, micronuclei in interphase cells (Ruffini Castiglione et al., 2011).

2.4. Histochemical detection of oxidative stress on root system

140   Five roots for each treatment were hand sectioned in correspondence to the initial root hair

141   area. Cross sections were immediately processed with specific staining reagents for

142   fluorescence and optical microscopy. Fluorescence microscope analysis was carried out with a

143   Leica DMLB, equipped with appropriate set of excitation/emission filters and with a Leica

144   DC300 ccd camera; optical microscope analysis was performed with a Leitz Diaplan,

145   equipped with a Leica DCF420 ccd camera. Fluorescent Amplex Ultrared® (Life

146   Technologies, USA) was applied for *in situ* detection of hydrogen peroxide (H_2O_2) following

147   manufacturing instructions. In brief, sections were incubated for 30 min at room temperature

148   (RT) in the dark in the staining mixture composed by 50 µl of 10mM Amplex Ultrared stock

149   solution in DMSO, 100 µl horseradish peroxidase (Sigma-Aldrich, USA) (10 U/ml in 0.05M

150   PB, pH 6), 4.85 ml of 0.05M PB pH 6. After three washes in the same buffer, the slices were

151   mounted in glycerol and observed with fluorescence microscope ($568_{ex}/681_{em}$ nm). Reactive

152   nitrogen species (RNS) were revealed by 2,3-Diaminonaphthalene staining (Life

153   Technologies, USA) dissolved in DMSO (0.5M) and then diluted 1:1000 in PBS 0.05M pH

154   6.8 just before the sample incubation in the dark at RT. After 30 min and three washes in the

155   same buffer, slices were mounted in glycerol for the observations with fluorescence

156   microscope ($365_{ex}/415_{em}$ nm). BODIPY® 581∕591 C11 was used as free radical sensor to

157   visualize lipid peroxidation levels as a change of the fluorescence emission peak from red to

158   green. The slices were incubated in 10 µM BODIPY in PBS 0.1M pH 7.4 for 30 min at RT in

159   the dark and then washed three times in the same buffer. Microscope evaluation was

160   performed acquiring simultaneously the green ($485_{ex}/510_{em}$ nm) and the red fluorescence

161   ($581_{ex}/591_{em}$ nm) signals and merging the two images (Kováčik et al., 2014). Endogenous

162   peroxidase activity was visualized under optical microscope exploiting a solution of

163   colourless guaiacol/H_2O_2 (5mM H_2O_2, 5mM guaiacol in 60mM PB pH 6.1) that became

164   dark/brown tetraguaiacol, due to peroxidase activity. After 10 min of incubation the slices

165   were washed three times in the same buffer and mounted in glycerol for microscope analysis

166   (Lepeduš et al., 2005).

167

168   *2.5. Determination of water content (WC) and of relative water content (RWC)*

169   Fresh weight (FW) was obtained by weighing the fresh roots. The roots were then

170   immersed in water overnight (turgid weight, TW), oven-dried at 100°C to constant weight

171   and reweighed (dry weight, DW).

172   WC percentage was estimated on the FW basis. RWC was determined as in Balestri et al.

173   (2014) and calculated with the formula:

174   RWC = [(FW-DW)/(TW-DW)] x 100

175

176   *2.6. Extraction and determination of H_2O_2 and thiobarbituric acid reactive substances*

177   *(TBARS)*

178   H_2O_2 content of roots was determined according to Jana and Choudhuri (1982). Roots

179   were ground and homogenised with phosphate buffer 50mM pH 6.5. The homogenate was

180   centrifuged at 6000g for 25 min. H_2O_2 content was determined using 0.1% titanium

181   chloride in 20% (v/v) H_2SO_4. The amount of H_2O_2 was detected spectrophotometrically

182   (410 nm), calculated from a standard curve and expressed as $\mu mol\ g^{-1}DW$.

183   Lipid peroxidation in roots was measured determining the amount of TBARS by the

184   thiobarbituric acid (TBA) reaction (Hartley-Whitaker et al., 2001) with minor

185   modifications. Roots were mixed with TBA reagent (10% w/v trichloroacetic acid + 0.25%

186   w/v thiobarbituric acid), heated (95°C for 30 min), cooled for 15 min and centrifuged at

187   2000g for 15 min. The level of TBARS was detected as specific absorbance at 532 nm by

188   subtracting the non-specific absorbance at 600 nm and calculated using an extinction

189 coefficient of 155mM^{-1} cm^{-1}. TBARS were expressed in nmol g^{-1} DW.

190

191 *2.7. Extraction and determination of proline*

192 Proline concentration was determined according to Bates (1973) with minor

193 modifications (Spanò et al., 2013). Root were homogenised with 3% sulfosalicylic acid.

194 The supernatant was incubated with glacial acetic acid and ninhydrin reagent (1:1:1) and

195 boiled at 100°C for 60 min. After cooling the reaction mixture, toluene was added and the

196 absorbance of toluene phase was read at 520 nm. Calculations were made on the base of a

197 standard curve and content was expressed as μmol g^{-1}DW.

198

199 *2.8. Extraction and determination of ascorbate and glutathione*

200 Ascorbate, reduced form (ASA) and oxidised form (dehydroascorbate, DHA), extraction

201 and determination were performed according to Spanò et al. (2011). Calculations were

202 made on the base of a standard curve. A blank was made in the absence of the extract and

203 content was expressed as μmol g^{-1}DW.

204 Glutathione was extracted and determined according to Gossett et al. (1994). Total

205 glutathione (reduced form, GSH + oxidised form, GSSG) was detected monitoring the rate

206 of change in absorbance at 412 nm. GSSG was determined after removal of GSH from the

207 extract by 2-vinylpyridine derivatization. GSH was detected by subtracting the amount of

208 GSSG from total glutathione and calculations were made on the base of a standard curve. A

209 blank was made in the absence of the extract and content was expressed as μmol g^{-1}DW.

210

211 *2.9. Enzyme extraction and assays*

212 Roots were ground in liquid nitrogen and the extraction was made at 4°C as in Spanò et

213 al. (2013). The homogenate was then centrifuged at 15000*g* for 20 min. For ascorbate

214 peroxidase, 2mM ascorbate was added to the extraction medium. Supernatants were

215 collected and stored in liquid nitrogen until their use for enzymatic assays.

216 Ascorbate peroxidase (APX, EC 1.11.1.11) activity was measured according to Nakano

217 & Asada (1981). Enzyme activity was assayed from the decrease in absorbance at 290 nm

218 (extinction coefficient $2.8mM^{-1}cm^{-1}$) as ascorbate was oxidised and enzyme extract

219 contained 25 µg protein ml^{-1}. Correction was made for the low, non-enzymatic oxidation of

220 ascorbate by H_2O_2 (blank).

221 Glutathione peroxidase (GPX, EC 1.11.1.9) activity was determined according to

222 Navari-Izzo et al. (1997) following the oxidation of NADPH at 340 nm (extinction

223 coefficient $6.2 mm^{-1} cm^{-1}$). Enzymatic extract contained 12.5 µg protein ml^{-1}.

224 Catalase (CAT, EC 1.11.1.6) activity was determined according to Aebi (1984).

225 Enzymatic extract contained 12.5 µg protein ml^{-1}. A blank containing only the enzymatic

226 solution was made. Specific activity was calculated from the $39.4mM^{-1} cm^{-1}$ extinction

227 coefficient.

228 Guaiacol peroxidase (POD, EC 1.11.1.7) activity was determined according to Arezky

229 et al. (2001) using 1% guaiacol as substrate. Enzymatic extract contained 5 µg protein ml^{-1}.

230 Enzymatic activity was determined following guaiacol oxidation by H_2O_2 (extinction

231 coefficient $26.6mM^{-1} cm^{-1}$) at 470 nm, one unit oxidising 1.0 µmole guaiacol per min.

232 All enzymatic activities were determined at 25°C and expressed as U g^{-1} protein. Protein

233 measurement was performed according to Bradford (1976), using BSA as standard.

234

235 *2.10. Statistical analysis*

236 All the data were the mean of at least three replicates from three independent experiments.

237 Statistical significance was determined by ANOVA tests followed by *post hoc* Bonferroni

238 multiple comparison test. *Post hoc* statistical significance is indicated in figures and tables

239   by different letters.

240

241   **3. Results**

242   *3.1. Germination and growth*

243   Germination percentage (Table 1) did not show significant differences between control

244   and treated materials. After 72 h germination roots from B treated seeds were significantly

245   shorter than P-NPs treated roots but not significantly different from C and S-NPs treated

246   materials (Fig. 1, Table 1). The highest VI (Table 1) was detected in P-NPs treated roots,

247   while the minimum value was characteristic of B treated samples.

248

249   *3.2. TEM observations*

250   The morphology of the TiO_2 P and S-NPs is shown in Figs 2a and 2b, respectively. Both

251   were extremely variable in electron density (Figs 2a, b). P-NPs were roughly round in shape

252   with a diameter from 2 to 12 nm (Fig. 2a). S-NPs had polyhedral shape and a wide size

253   distribution ranging from 10 to 100 nm (Fig. 2b). Sections of control roots showed cells with

254   large vacuoles with scanty materials evident. The cytoplasm was rich in well structured

255   organelles, particularly long rough endoplasmic reticulum cisternae, dictyosomes,

256   mitochondria and plastids (Fig. 2c). The cell ultrastructure of P-NPs treated roots appeared

257   similar to control ones. The only noteworthy difference was the presence of electron dense

258   particles embedded in scanty electron dense material scattered in the cell vacuole (Fig. 2d).

259   Often dense particles of 5-12 nm were observed crossing the walls of rhizodermis and of root

260   parenchyma cells (Figs 2e, f).

261   The S-NPs treated roots showed cell vacuoles containing single or aggregated NPs (Fig.

262   3a). Several cells showed wide zone of cytoplasmic degeneration (Fig. 3b) often surrounded

263   by a double membrane. In these cytoplasmic portions a large number of small and/or large

264 vesicles with rough membranes and NPs of polyedric form, isolated or aggregated, were

265 observed (Fig. 3b). Some of these cells showed more or less evident plasmalemma-wall

266 detachment as in plasmolysis (data not shown). In the cell walls of rhizodermis numerous

267 aggregates (60-120 nm) of dense particles were often present (Fig. 3c). Numerous vesicles,

268 smooth endoplasmic reticulum cisternae and organelles, often not well recognizable, were

269 present in the cells of the B treated roots (Fig. 3d). Some cells showed nuclei with extremely

270 disperse chromatin and wide portion of cytoplasmic degeneration (Fig. 3e). Furthermore, a

271 great number of cells evidenced an amazing electron dense cytoplasm with numerous not well

272 recognizable organelles (probably plastids), amyloplasts and weakly electron opaque bodies

273 of about 0.3- 0.5 µm in diameter (Fig. 3f).

274

275 *3.3. Cytological evaluation of the root meristem*

276   The mitotic activity (MI) and the occurrence of micronuclei in interphase (MNC),

277 evidenced not significant disturbances under different treatments. On the contrary, when the

278 frequency of anomalies and/or aberrations (AI) in dividing cells were recorded, a significant

279 increase in the AI was observed for the samples S and B, while the mean value of the AI in

280 the samples P was not statistically different from the control (Fig. 4). Fig. 5 shows some

281 representatives examples of the scored mitotic abnormalities.

282

283 *3.4. Histological evaluation associated to in situ detection of oxidative stress*

284   Probes specific for H_2O_2, RNS, lipid peroxidation and guaiacol-peroxidase activity (Fig. 6)

285 directly detect qualitative signals related to oxidative stress. In cross sections of control and

286 treated roots the signal obtained with the fluorescent probe Amplex H_2O_2, apart from a faint

287 staining involving the cortical area, was mainly localized in xylem vessels (Fig. 6a). In the

288 samples treated with both the types of NPs we observed a general increase of H_2O_2 in the

289   vascular cylinder involving as well the phloem, alternated between the arms of the xylem

290   (Figs 6b, c). On the contrary, the roots treated with bulk material showed a strong staining in

291   the rhizodermis and in the periphery of the cortical cylinder (Fig. 6d).

292   Concerning the RNS, the control root presented a distinctive blue staining involving

293   mainly the xylem vessels, and, to a lesser extent, the region surrounding the stele and the

294   peripheral area of the cortex (Fig. 6e). Under treatments, we observed a general increase of

295   the fluorescence intensity in respect to the control, especially in the samples S and B (Figs 6f,

296   g, h). Sample B was the most reactive also at the BODIPY fluorescent probe (Fig. 6l), which

297   identified lipid peroxidation as a change of the fluorescence emission peak from red to green.

298   In this sample the green fluorescence was observed in all the root tissues, with the exception

299   of the central part of the stele. Samples P and S (Figs 6j, k) were similar to the control (Fig.

300   6i) as to the intensity of the staining in the root cortex, but a well defined green area

301   corresponding to the perycicle and to the outermost cells of vascular tissues was observed in

302   sample S (Fig. 6k). Figs 6m-p shows representative sections after guaiacol staining. The

303   brown colour indicates peroxidase activity induced by treatments. Root cross sections were

304   lightly stained in samples C and P (Figs 6m, n), the former showing a more diffuse signal, the

305   latter being more sharply stained, also in the area of phloem arcs. Guaiacol reaction strongly

306   increased in the S and B samples (Figs 6o, p).

307

308   *3.5. Water content and relative water content*

309   Bulk-treated material was characterized by the highest values of both WC and RWC (Table

310   1). Roots of NPs-treated samples, on the other hand, showed all similar hydric status.

311

312   *3.6. H_2O_2 and TBARS*

313   The highest contents of H_2O_2 and TBARS (Table 1) were detected in B roots. H_2O_2

314   concentration was lower in C roots and even more in S samples, showing the lowest value in

315   P-NPs treated material. Both NPs-treated roots had TBARS content not significantly different

316   from C roots.

317

318   *3.7. Proline and low molecular weight antioxidants*

319   Proline (Table 1) had the highest value in C roots, was significantly lower in B and even

320   more in NPs-treated seeds, regardless of the type of NPs used. B roots were characterized by

321   the highest contents of both total ascorbate and glutathione (Table 1). P-NPs treated roots

322   showed the lowest values of these low molecular weight antioxidants, while S roots did not

323   differ significantly from control material. Interestingly, the highest values of reducing power

324   of ASA/DHA couples were characteristic of NPs-treated roots. Significantly high was the

325   GSH/GSSG ratio in sample P (Table 1).

326

327   *3.8. Antioxidant enzymes*

328   Although no significant difference was observed in GPX activity among different

329   treatments, both APX and CAT activities were significantly lower in all treated roots,

330   regardless of the type of treatment (Table 1). The highest POD activity was detected in S-NPs

331   treated roots, significantly lower values in B then in C samples and the lowest activity in P-

332   NPs treated samples.

333

334   **4. Discussion**

335   NPs can influence plant growth and development without being internalized (Asli and

336   Neumann, 2009) or directly entering plant cells by means of different penetration mechanisms

337   (Chichiriccò and Poma, 2015), also when they have dimensions higher than cell wall pore

338   exclusion limit (Larue et al., 2012). However, few literature data are available concerning the

339   effects of TiO$_2$-NPs and bulk material on root ultrastucture. The present ultrastructural

340   observations confirmed the presence of TiO$_2$-NPs inside *V. faba* root cells and provided

341   significant information on their effects. The NPs penetrated through the cell walls of

342   rhizodermis and moved via the apoplast pathway. Indeed they were observed in the P-NPs

343   treated root wall generally as individual particles, while the S-NPs crossed the rhizodermis

344   walls as aggregates. The wall pore size can allow the diffusion of molecules (exceptionally)

345   up to 10 nm of diameter (Larue et al., 2012), as a consequence the P-NPs can cross the

346   rhizodermis and move through the apoplasm. It was supposed a NPs induction of hydroxyl

347   radicals that can loose the wall with enlargement of pores by cleavage of pectin-

348   polysaccharides (Kim et al., 2014; Larue et al., 2012). In this way it is possible to explain the

349   wall penetration of the large particles and of S-NPs aggregates. The vacuolar sequestration of

350   P-NPs allows to avoid interaction of particles with organelles and metabolic process. The

351   success of this detoxification mechanism is attested by the fact that the cell ultrastructure of

352   P-NPs treated roots appeared similar to the control ones. On the contrary, in S-NPs treated

353   roots the NPs were localized both in the vacuoles and in wide zones of degenerated

354   cytoplasm, often surrounded by a double membrane. These findings recall the double

355   membrane autophagosomes that form in response to biotic and abiotic stress and can bring to

356   programmed cell death (Kutik et al., 2014). This process is characterized by gradual lysis of

357   the cellular content leaving at the end the hollow cell wall shell (Kutik et al., 2014).

358   Therefore, in *V. faba* the damage of the cell ultrastructure appeared to be related to size and

359   shape of NPs. B treatment strongly affected cell ultrastructure, as electron dense cytoplasm

360   and numerous not well recognizable organelles (probably plastids), amyloplasts, and weakly

361   electron opaque bodies of about 0.3-0.5 µm diameter were observed, giving the appearance of

362   not yet differentiated embryo cells.

363   Contrasting results were reported about the effects of TiO$_2$-NPs on plant germination and

364 growth (Ghosh et al., 2010; Ruffini Castiglione et al., 2011, 2014; Seeger et al., 2009; Song et

365 al., 2013). In *V. faba* the different treatments of TiO_2-NPs and bulk material did not cause

366 germination inhibition, but bulk material induced the production of seedlings with the shortest

367 roots. This is in contrast with Azimi et al. (2013) who reported no variation in root length in

368 seeds of *Agropyron desertorum* treated with similar concentrations of bulk TiO_2. Additional

369 interesting information can derive from VI, which, summarizing the impact of a particular

370 compound on seed germination and seedling growth, can give an idea of the whole

371 germination process (Ruffini Castiglione et al., 2014). Our previous data on another species of

372 *Vicia* revealed a phytotoxic effect only at the highest (4‰) S-NPs concentration. In

373 accordance, *V. faba* treated with low concentrations of S-NPs had a VI comparable with that

374 of C material. The increase in VI induced by P-NPs was in accordance with reports by Feizi et

375 al. (2013) for sage underlining a different action of NPs in function of the size and shape.

376 Despite the minor root growth, B-treated plants were characterized by a good hydric status, as

377 indicated by WC and RWC, showing that the impaired root growth was not due to tissue

378 water deficit.

379   DNA injuries and genotoxic effects were demonstrated after TiO_2-NPs treatments both in

380 animal (Shukla et al., 2013) and in plant systems (Ghosh et al., 2010; Ruffini Castiglione et

381 al., 2011, 2014; Moreno-Olivas et al., 2014; Pakrashi et al., 2014) by different experimental

382 approaches such as comet assay, chromosomal aberration analysis, micronuclei assay, γ-

383 H2AX assay, DNA laddering assay and RAPD analysis.

384   Concerning cytological evaluation of the root meristem behaviour, in contrast to what was

385 observed in the root apex following plant treatments with nano- and macroscale metals

386 (Kumari et al., 2009; Balestri et al., 2014), no negative effect was registered for the mitotic

387 activity in our experimental conditions: all the recorded MI were not significantly different

388 from the control, indicating absence of cytotoxicity for all the treatments. Also the MNC,

389   recently standardized for *V. faba* by an international protocol, ISO 29200 (Cotelle et al.,

390   2015), did not reveal toxic effects on root apex. In this plant system, the absence of

391   micronuclei induction occurred in parallel with an increase in the frequency of AI in samples

392   S and B. The lack of concordance between MNC test and AI in these two treatments indicated

393   that S-NPs and the bulk counterpart could act as indirect toxicants and/or exert on

394   meristematic cells a delayed effect along 72 hours of treatment, allowing to detect only

395   anomalies and/or aberrations in dividing cells but not the resulting micronuclei in the

396   subsequent interphase. Genotoxic effects of S-NPs were already observed on *V. narbonensis*

397   and *Zea mays* (Ruffini Castiglione et al., 2011) at higher concentrations (200-4000 mg/L);

398   besides bulk material provoked a genotoxic response in *Allium cepa* at about 100 mg/L and

399   above (Ghosh et al., 2010).

400   The genotoxicity of NPs, supposed to be due to oxidative stress as the primary key

401   mechanism inducing DNA damages, strongly coupled to ROS activity and to depletion of cell

402   antioxidant response. ROS, such as superoxide, H_2O_2 and hydroxyl radicals may act as

403   elicitors of common stress response (Mittler, 2002); however when they accumulate at critical

404   level an oxidative stress can ensue (Parida and Das, 2005). Nevertheless, H_2O_2 may act as an

405   active regulator of biological processes related to growth and differentiation (Bellani et al.,

406   2012), as observed in tracheary elements and in endodermis of the control and all the treated

407   samples.

408   Previous studies showed that NPs can induce both increase (Zhao et al., 2012) and

409   decrease (Sharma et al., 2012) in H_2O_2 content, even in the same species in a NPs

410   concentration-dependent manner (Ruffini Castiglione et al., 2014). In our experimental

411   conditions, in accordance with data on *Cicer arietinum* (Mohammadi et al., 2014), TiO_2-NPs

412   induced a significant decrease in the content of this molecule, the lowest value characterizing

413   P-NPs treated roots. The low H_2O_2 content for P and S-NPs treated materials could be due at

414   least in part to a possible radical scavenging activity of TiO_2-NPs, higher at the decrease in

415   particle size and increase in surface area (Kalyanasundharam and Prakash, 2015). This

416   scavenging role could be very helpful in increasing plant tolerance under stress condition

417   (Mohammadi et al., 2014). Roots treated with P and S-NPs showed a peculiar staining pattern

418   of H_2O_2 in different root compartments, involving mainly the vascular cylinder and the

419   phloem arcs: this H_2O_2 localization may be allied to a different root response elicited by the

420   nanomaterials. The highest content of H_2O_2 was detected in the rhizodermis and in the

421   peripheral cortex of bulk-treated seedlings. This could be related to lignification processes as

422   resistance mechanism promoting plant defence (Moura et al., 2010).

423   With histochemical approach, lipid peroxidation was strongly and diffusely detectable in

424   B treated samples, as confirmed by TBARS assay, indicative of membrane damage, mainly in

425   root cortex. In this material the good correlation between TBARS and H_2O_2 content could

426   indicate an H_2O_2-dependent membrane damage. These data are in line with ultrastructural

427   observations on B treated samples. NPs treatments induced, in accordance with biochemical

428   data, a whole signal comparable to the control, apart from a peculiar staining pattern in the

429   outermost layers of vascular cylinder characteristics for the S-NPs. The lack of membrane

430   damage in NPs-treated materials and C roots is in accordance with previous data on *V.*

431   *narbonensis* treated with higher S-NPs concentrations (Ruffini Castiglione et al., 2014).

432   Therefore, *V. faba* root seems to be strongly harmed by bulk material treatment while TiO_2 S-

433   NPs may act inducing a localized tissue-specific membrane damage. To protect cellular

434   structure and metabolism from oxidative damage, plant evolved a complex enzymatic and non

435   enzymatic system. Proline can contribute along with ascorbate and glutathione to ROS

436   detoxification. Given the lower proline content in treated seedlings than in control ones, the

437   main antioxidant roles were played in our conditions by ascorbate and glutathione in

438   accordance with literature (Jiang et al., 2014). The higher pools of both ascorbate and

439   glutathione in bulk-treated material showed the importance of these antioxidants in oxidative

440   stress response. The highest reducing power recorded in NPs-treated roots was in line with the

441   low H_2O_2 content detected in these materials.

442   Enzymatic activities were generally inhibited in treated seedlings, with the exception of

443   GPX characterized by similar activities in all materials. The decrease in CAT activity detected

444   in NPs-treated roots was also relieved in onion seedlings treated with TiO_2-NPs of size similar

445   to that of our P material (Laware and Raskar, 2014) showing the particular sensitivity of this

446   enzyme to TiO_2-NPs. Our results highlighted a different POD activity in dependence from

447   NPs size: in particular the maximum value was observed in S-treated roots, confirming

448   previous data obtained in *V. narbonensis* under different concentrations of the same NPs

449   (Ruffini Castiglione et al., 2014), while in P-NPs roots POD activity was lower than in control

450   roots. These results were basically comparable to those obtained *in situ* by guaiacol-

451   peroxidase staining, resembling the recorded pattern of H_2O_2 staining with a specific

452   involvement of the phloem tissues for the samples treated with both TiO_2-NPs. Guaiacol

453   peroxidase activity, known as having important roles in control of growth by lignification

454   (Gaspar et al., 1991), was stronger in xylem vessels under all the treatments, indicating a

455   precocious status of tracheary element differentiation in respect to the control. This process

456   seems to be more pronounced in the treatments with S-NPs and B material as further

457   confirmed by the localization of RNS, among which NO is involved as signal molecule, in

458   plant cell differentiation, xylogenesis and cell wall lignification (Planchet and Kaiser, 2006).

459

460   **5. Conclusions**

461   On the whole, the low concentration of the different materials was able to induce specific

462   responses in our plant model system. Germination process was stimulated in P-NPs treated

463   seeds. TiO_2, supplied as bulk material, induced oxidative stress, in terms of both H_2O_2 and

464   TBARS content, disturbance in root growth and in cellular ultrastructure. Genotoxic effects,

465   detectable in bulk treated roots, were however also evident following S-NPs treatment.

466   In addition *in situ* analysis revealed localized stress signals in specific root compartments

467   related to developmental and/or defence response, typical for the different treatments. In bulk-

468   treated roots antioxidant defence seemed to rely mainly on low molecular weight

469   antioxidants. In the different NPs-treatments a high reducing power of glutathione in P-NPs

470   treated seedlings and a high POD activity in S-NPs treated material were observed. The

471   activation of the antioxidant response in the presence of low levels of H_2O_2 is particularly

472   interesting as it could help to explain the protective action of TiO_2-NPs in plants subjected to

473   abiotic stress. These results all together suggest that TiO_2-NPs, able to penetrate into root

474   cells, may exert different actions depending on their size and their shape and that the bulk

475   counterpart, in our experimental conditions, seems to provoke the major adverse effects in *V.*

476   *faba* roots.

477

478

483 **References**

484

485 Aebi, H., 1984. Catalase *in vitro*. Meth. Enzym. 105, 121-126.

486 Arezky, O., Boxus, P., Kevers, C., Gaspar, T., 2001. Changes in peroxidase activity, and

487   level of phenolic compounds during light-induced plantlet regeneration from

488   *Eucalyptus camaldulensis* Dhen. nodes *in vitro*. Plant Growth Regul. 33, 215-219.

489 Asli, S., Neumann, P.M., 2009. Colloidal suspensions of clay or titanium dioxide

490   nanoparticles can inhibit leaf growth and transpiration via physical effects on root

491   water transport. Plant Cell Environ. 32, 577-584.

492 Azimi, R., Feizi, H., Khajeh Hosseini, M., 2013. Can bulk and nanosized titanium dioxide

493   particles improve germination features of wheatgrass (*Agropyron desertorum*). Not.

494   Sci. Biol. 5, 325-331.

495 Baderna, D., Lomazzi, E., Pogliaghi, A., Ciaccia G., Lodi M., Benfenati, E. 2015. Acute

496   phytotoxicity of seven metals alone and in mixture: are Italian soil threshold

497   concentrations suitable for plant protection? Environ. Res. 40, 102–111.

498 Balestri, M., Ceccarini, A., Forino L.M.C., Zelko, I., Martinka, M.,·Lux, A., Ruffini

499   Castiglione, M., 2014. Cadmium uptake, localization and stress ‐induced morphogenic

500   response in the fern *Pteris vittata*. Planta 239, 1055-1064.

501 Balestri, M., Bottega, S., Spanò, C., 2014. Response of *Pteris vittata* to different cadmium

502   treatments. Acta Physiol. Plant. 36, 767-775.

503 Bates, L.S., 1973. Rapid determination of free proline for water-stress studies. Plant Soil

504   39, 205-207.

505 Bellani, L.M., Salvini, L., Dell'Aquila, A., Scialabba, A., 2012. Reactive oxygen species

506   release, vitamin E, fatty acid and phytosterol contents of artificially aged radish

507   (*Raphanus sativus* L.) seeds during germination. Acta Physiol. Plant. 34, 1789-1799.

508   Bhawana, P., Fulekar, M.H., 2012. Nanotechnology: remediation technologies to clean up

509   the environmental pollutants. Res. J. Chem. Sci. 2, 90-96.

510   Bradford, M., 1976. A rapid and sensitive method for the quantitation of microgram

511   quantities of protein utilizing the principle of protein-dye binding. Anal. Biochem. 72,

512   248-254.

513   Chichiriccò, G, Poma, A., 2015. Penetration and toxicity of nanomaterials in higher plants.

514   Nanomaterials 5, 851-873.

515   Chuankrerkkul, N., Sangsuk, S., 2008. Current status of nanotechnology consumer

516   products and nano-safety issues. J. Min. Met. Mat. Soc. 18, 75-79.

517   Cotelle, S., Dhyèvre, A., Muller, S., Chenon, P., Manier, N., Pandard, P., Echairi, A.,

518   Silvestre, J., Guiresse, M., Pinelli, E., Giorgetti, L., Barbafieri, M., Engel, F., Radetski,

519   C.M., 2015. Soil genotoxicity assessment-results of an interlaboratory study on the

520   *Vicia* micronucleus assay in the context of ISO standardization. Environ. Sci. Pollut.

521   Res. Int. 22, 988-995.

522   Du, W., Sun, Y., Ji, R., Zhu, J., Wu, J., Guo, H., 2011. TiO_2 and ZnO nanoparticles

523   negatively affect wheat growth and soil enzyme activities in agricultural soil. J.

524   Environ. Monit. 13, 822-828.

525   Feizi, H., Shahram, A., Farzin, A., Saeed, J.P., 2013. Comparative effects of nanosized and

526   bulk titanium dioxide concentrations on medicinal plant *Salvia officinalis* L. Ann. Rev.

527   Res. Biol. 3, 814-824.

528   Frazier, T.P., Burklew, C.E., Zhang, B., 2014. Titanium dioxide nanoparticles affect the

529   growth and microRNA expression of tobacco (*Nicotiana tabacum*). Funct. Integr.

530   Genomics 14, 75-83.

531   Gaspar, T.H., Penel, C., Hagege, D., Greppin, H., 1991. Peroxidases in plant growth,

532   differentiation and development processes, in: Lobarzewski, J., Greppin, H., Penel, C.,

533   Gaspar, T.H. (Eds.), Biochemical, Molecular and physiological aspects of plant

534   peroxidases. Université de Genève, pp. 249-280.

535   Ghosh, M., Bandyopadhyay, M., Mukherjee, A., 2010. Genotoxicity of titanium dioxide

536   (TiO_2) NPs at two trophic levels: plant and human lymphocytes. Chemosphere 81,

537   1253-1262.

538   Giorgetti, E., Muniz Miranda, M., Caporali, S., Canton, P., Marsilia, P., Vergari, C.,

539   Giammanco, F., 2014. TiO_2 nanoparticles obtained by laser ablation in water: Influence

540   of pulse energy and duration on the crystalline phase. J. Alloy Compd. 643, S75-S79.

541   Giorgetti, L., Ruffini Castiglione, M., Bernabini, M., Geri, C., 2011. Nanoparticles effects on

542   growth and differentiation in cell culture of carrot (*Daucus carota* L.). Agrochimica 55,

543   45-53.

544   Giorgetti, L., Ruffini Castiglione, M., 2016. Oil palm *in vitro* regeneration:

545   microdensitometric analysis during reproduction and development. Caryologia, on line

546   first, DOI: 10.1080/00087114.2015.1109953

547   Gossett, D.R., Millhollon, E.P., Lucas, M.C., 1994. Antioxidant response to NaCl stress in

548   salt-tolerant and salt-sensitive cultivars of cotton. Crop Sci. 34, 706-714.

549   Hartley-Whitaker, J., Ainsworth, G., Meharg, A.A., 2001. Copper- and arsenate-induced

550   oxidative stress in *Holcus lanatus* L. clones with differential sensitivity. Plant Cell

551   Environ. 24, 713-722.

552   Hotze, E.M., Phenrat, T., Lowry, G.V., 2010. Nanoparticle aggregation: challenges to

553   understanding transport and reactivity in the environment. J. Environ. Qual. 39, 1909–

554   1924

555   IARC - International Agency for Research on Cancer, 2010. Monographs 93. Titanium

556   Dioxide. http://monographs.iarc.fr/ENG/Monographs/vol93/mono93-7.pdf

557   Jana, S., Choudhuri, M.A., 1982. Glycolate metabolism of three submerged aquatic

558   angiosperm during aging. Aquat. Bot. 12, 345-354.

559   Jiang, H.S, Qiu, X.N., Li, G.B., Li, W., Yin, L.Y., 2014. Silver nanoparticles induced

560   accumulation of reactive oxygen species and alteration of antioxidant systems in the

561   aquatic plant *Spirodela polyrhiza.* Environ. Toxicol. Chem. 33, 1398-1405.

562   Kalyanasundharam, S., Prakash, M.J., 2015. Biosynthesis and characterization of titanium

563   dioxide nanoparticles using *Pithecellobium dulce* and *Lagenaria siceraria* aqueous leaf

564   extract and screening their free radical scavenging and antibacterial properties. Int.

565   Lett. Chem. Phys. Astron. 50, 80-95.

566   Karnovsky, M.J., 1965. A formaldehyde-glutaraldehyde fixative of high osmolality for use

567   in electron microscopy. J. Cell Biol. 27, 137-138.

568   Kaveh, R., Li, Y.S., Ranjbar, S., Tehrani, R., Brueck, C.L., Van Aken, B., 2013. Changes in

569   *Arabidopsis thaliana* gene expression in response to silver nanoparticles and silver ions.

570   Environ. Sci. Technol. 47, 10637-10644.

571   Kim, J.H., Lee, Y., Kim, E.J., Gu, S., Sohn, E.J., Seo, Y.S., An, H.J., Chang, Y.S., 2014.

572   Exposure of iron nanoparticles to *Arabidopsis thaliana* enhances root elongation by

573   triggering cell wall loosening. Environ. Sci. Technol. 48, 3477-3485.

574   Kováčik, J., Babula, P., Hedbavny, J., Švec, P., 2014. Manganese-induced oxidative stress

575   in two ontogenetic stages of chamomile and amelioration by nitric oxide. Plant Sci.

576   215-216, 1-10.

577   Kumari, M., Mukherjee, A., Chandrasekaran, N., 2009. Genotoxicity of silver

578   nanoparticles in *Allium cepa*. Sci. Total Environ. 407, 5243-5246.

579   Kutik, J., Kuthanova, A., Smertenko, A., Fischer, L., Opatrny, Z., 2014. Cadmium-induced

580   cell death in BY-2 cell structure starts with vacuolization of cytoplasm and terminates

581   with necrosis. Physiol. Plant. 151, 423-433.

582 Larue, C., Laurette, J., Herlin-Boime, N., Khodja, H., Fayard, B., Flank, A.M., Brisset, F.,

583   Carriere, M., 2012. Accumulation, translocation and impact of TiO_2 nanoparticles in

584   wheat (*Triticum aestivum* spp.): influence of diameter and crystal phase. Sci. Total

585   Environ. 431, 197-208.

586 Laware, S.L., Raskar, S., 2014. Effect of titanium dioxide nanoparticles on hydrolytic and

587   antioxidant enzymes during seed germination in onion. Int. J. Curr. Microbiol. Appl.

588   Sci. 3, 749-760.

589 Lepeduš, H., Jozić, M., Štolfa, I., Pavičić, N., Hackenbereger, K., Cesar, V., 2005. Changes

590   in peroxidase activity in the peel of Unshiu Mandarin (*Citrus unshiu* Marc.) fruit with

591   different storage treatments. Food Technol. Biotech. 43, 71-77.

592 Liu, W.K., 2011. TiO_2-NPs application in agriculture: a review, in Hendriks, B.P. (Ed.),

593   Agricultural research updates. Nova Publisher, Hauppage, New York, pp. 137-145.

594 Ma, X., Geiser-Lee, J., Deng, Y., Kolmakov, A., 2010. Interactions between engineered

595   nanoparticles (ENPs) and plants: Phytotoxicity, uptake and accumulation. Sci. Total

596   Environ. 408, 3053-3061.

597 Mittler, R., 2002. Oxidative stress, antioxidants and stress tolerance. Trends Plant Sci. 7,

598   405-410.

599 Mohammadi, R., Maali-Amiri, R., Mantri, N.L., 2014. Effect of TiO_2 nanoparticles on

600   oxidative damage and antioxidant defense systems in chickpea seedlings during cold

601   stress. Russ. J. Plant Physiol. 61, 768-775.

602 Moreno-Olivas, F., Gant Jr., V.U., Johnson, K.L., Peralta-Videa, J.R., Gardea-Torresdey,

603   J.L., 2014. Random amplified polymorphic DNA reveals that TiO_2 nanoparticles are

604   genotoxic to *Cucurbita pepo*. J. Zhejiang Univ.-SCI. A 15, 618-623.

605 Moura, J.C.M.S., Bonine, C.A.V., de Oliveira Fernandes Viana, J., Carnier Dornelas, M.,

606   Mazzafera, P., 2010. Abiotic and biotic stresses and changes in the lignin content and

607   composition in plants. J. Integr. Plant Biol. 52, 360-376.

608   Nakano, Y., Asada, K., 1981. Hydrogen peroxide is scavenged by ascorbate-specific

609   peroxidase in spinach chloroplasts. Plant Cell Physiol. 22, 867-880.

610   Navari-Izzo, F., Meneguzzo, S., Loggini, B., Vazzana, C., Sgherri, C.L.M., 1997. The role

611   of the glutathione system during dehydration of *Boea hygroscopica*. Physiol. Plant. 99,

612   23-30.

613   Navarro, E., Baun, A., Behra, R., Hartmann, N.B., Filser, J., Miao, A.J., Quigg, A.,

614   Santschi, P.H., Sigg, L., 2008. Environmental behavior and ecotoxicity of engineered

615   nanoparticles to algae, plants, and fungi. Ecotoxicology 17, 372-386.

616   Ortlieb, M., 2010. White giant or white Dwarf? Particle size distribution measurements of

617   TiO_2. GIT Lab. J. Eur. 14, 42-43.

618   Pakrashi, S., Jain, N., Dalai, S., Jayakumar, J., Chandrasekaran, P.T., Raichur, A.M.,

619   Chandrasekaran, N., Mukherjee, A., 2014. *In vivo* genotoxicity assessment of titanium

620   dioxide nanoparticles by *Allium cepa* root tip assay at high exposure concentrations.

621   Plos One 9, e87789.

622   Parida, A.K., Das, A.B., 2005. Salt tolerance and salinity effects on plants: a review.

623   Ecotox. Environ. Safety 60, 324-349.

624   Planchet, P., Kaiser, W.M., 2006. Nitric oxide production in plants. Plant. Signal. Behav. 1,

625   46-51.

626   Poborilova, Z., Opatrilova, R., Babula, P., 2013. Toxicity of aluminium oxide nanoparticles

627   demonstrated using a BY-2 plant cell suspension culture model. Environ. Exp. Bot. 91, 1-

628   11.

629   Praetorius, A., Scheringer, M., Hungerbühler, K., 2012. Development of environmental fate

630   models for engineered nanoparticles: a case study of TiO_2 nanoparticles in the Rhine

631   river. Environ. Sci. Technol. 46, 6705-6713.

632 Raliya, R., Biswas, P., Tarafdar, J.C., 2015. TiO$_2$ nanoparticle biosynthesis and its

633   physiological effect on mung bean (*Vigna radiata* L.). Biotech. Rep. 5, 22-26.

634 Ruffini Castiglione, M., Cremonini, R., 2009. Nanoparticles and higher plants. Caryologia 62,

635   161-165.

636 Ruffini Castiglione, M., Giorgetti, L., Cremonini, R., Bottega, S., Spanò, C., 2014. Impact

637   of TiO$_2$ nanoparticles on *Vicia narbonensis* L.: potential toxicity effects. Protoplasma

638   251, 1471-1479.

639 Ruffini Castiglione, M., Giorgetti, L., Geri, C., Cremonini, R., 2011. The effects of nano-

640   TiO$_2$ on seed germination, development and mitosis of root tip cells of *Vicia*

641   *narbonensis* L. and *Zea mays* L. J. Nanopart. Res. 13, 2443-2449.

642 Seeger, E.M., Buan, A., Kästner, M., Trapp, S., 2009. Insignificant acute toxicity of TiO$_2$

643   NPs to willow trees. J. Soils Sediments 9, 46-53.

644 Sharma, P., Bhatt, D., Zaidi, M.G.H., Saradhi, P.P., Khanna, P.K., Arora, S., 2012. Silver

645   nanoparticle-mediated enhancement in growth and antioxidant status of *Brassica*

646   *juncea*. Appl. Biochem. Biotechnol. 167, 2225-2233.

647 Song, U., Shin, M., Lee, G., Roh, J., Kim, Y., Lee, E.J., 2013. Functional analysis of TiO$_2$

648   nanoparticle toxicity in three plant species. Biol. Trace Elem. Res. 155, 93-103.

649 Spanò, C., Bottega, S., Lorenzi, R., Grilli, I., 2011. Ageing in embryos from wheat grains

650   stored at different temperatures: oxidative stress and antioxidant response. Funct. Plant

651   Biol. 38, 624-631.

652 Spanò, C., Bruno, M., Bottega, S., 2013. *Calystegia soldanella*: dune versus laboratory

653   plants to highlight key adaptive physiological traits. Acta Physiol. Plant. 35, 1329-

654   1336.

655   Shukla, R.K., Kumar, A., Gurbani, D., Pandey, A.K., Singh, S., Dhawan, A., 2013. TiO_2

656   nanoparticles induce oxidative DNA damage and apoptosis in human liver cells.

657   Nanotoxicology 7, 48-60.

658   USEPA (U.S. Environ Protection Agency), 2010. Emerging contaminants-nanomaterials.

659   http://www.epa.gov/region9/mediacenter/nano-ucla/emerging_contaminant_nanomaterials.pdf

660   Zhao, L., Peng, B., Hernandez-Viezcas, J.A., Rico, C., Sun, Y., Peralta-Videa, J.R., Tang,

661   X., Niu, L., Jin, L., Varela-Ramirez, A., Zhang, J., Gardea-Torresdey, J.L., 2012. Stress

662   response and tolerance of *Zea mays* to CeO_2 nanoparticles: cross talk among H_2O_2, heat

663   shock protein, and lipid peroxidation. ACS Nano 6, 9615-9622.

664   Zheng, L., Hong, F., Lu, S., Liu, C., 2005. Effect of TiO_2-NPs on strength of naturally aged

665   seeds and growth of spinach. Biol Trace Elem Res 104, 83-92.

666

Figure captions

668

669   **Fig. 1.** *V. faba* seedlings. Representative samples after 72h germination in water (control), in

670   the presence of 50mg/L of TiO$_2$ P-NPs, S-NPs and bulk counterpart (Bulk).

671

672   **Fig. 2.** TEM images of (a) P-NPs (arrows) and (b) S-NPs (arrows). (c) Cell portion of control

673   *V. faba* root. The arrow indicates rough endoplasmic reticulum. (d, e) Cell portions of P-NPs

674   treated roots. The arrows indicate P-NPs. (f) P-NPs in two rhizodermis cell walls (arrows). c,

675   chromatin; m, mitochondria; n, nucleolus; v, vacuole; w, rhizodermis cell wall.

676

677   **Fig. 3.** TEM images of (a) aggregate of NPs (arrows) in the vacuole of S-NPs treated root

678   cell. (b) S-NPs (arrows) in portion of degenerated cytoplasm. The double arrows indicate

679   vesicles with rough membranes; the arrowheads indicate vesicles. (c) Aggregates of S-NPs

680   (arrows) in the rhizodermis cell wall. (d-f) Portions of cells of B treated roots. The arrows

681   indicate smooth endoplasmic reticulum. n, nucleus; dc, degenerated cytoplasm; o, not well

682   recognizable organelles; b, weakly electron opaque bodies; w, rhizodermis cell wall.

683

684   **Fig. 4.** Different behaviour of *V. faba* root apex. Mean values of mitotic index (MI %),

685   aberration index (AI %) and of micronuclei frequency (MNC ‰) recorded after 72h

686   germination in water (control), in the presence of 50mg/L of TiO$_2$ P-NPs, S-NPs and bulk

687   counterpart (Bulk). Bars represent standard errors. Different letters, within each analyzed

688   parameter, indicate significant differences by Bonferroni's multiple comparison test ($p <$

689   0.05).

690

691   **Fig. 5**. Representative mitotic abnormalities in TiO$_2$ S-NPs and Bulk treatments in *V. faba* root

692   tip meristem. (a) Micronuclei; (b-c) sticky chromosomes; (d) laggard chromosome in early

693   anaphase; (e-f) C metaphases; (g) somatic pairing; (h-i) reduction grouping; (j) laggard

694   chromosome in disturbed anaphase; (k-m) chromosome bridges in anaphases.

695

696   **Fig. 6.** Cross hand sections of *V. faba* roots of seedlings after 72h germination in water

697   (control), in the presence of 50mg/L of TiO$_2$ P-NPs, S-NPs and bulk counterpart (Bulk).

698   The plate comprehends representative images of *in situ* detection of H$_2$O$_2$, of reactive nitrogen

699   species (RNS), lipid peroxidation (Lipid perox) and peroxidase activity (POD activity). Bars

700   indicate 200 µm.

701

Table 1. Growth and physiological parameters in *Vicia faba* roots of seedlings after 72h of germination in water (control), in the presence of TiO$_2$ Plasma Tech (P-NPs), Sigma (S-NPs) and bulk counterpart (Bulk). Relative water content (RWC), thiobarbituric acid reactive substances (TBARS), total ascorbate (reduced ascorbate, ASA + dehydroascorbate, DHA), total glutathione (reduced form, GSH + oxidised form, GSSG), ascorbate peroxidase (APX), glutathione peroxidase (GPX), guaiacol peroxidase (POD) and catalase (CAT).

708

	Control	Bulk	TiO$_2$ P-NPs	TiO$_2$ S-NPs
Germination (%)	86.67±4.25a	86.67±2.04a	91.67±3.73a	89.58±2.08a
Root length (mm)	46.62±1.41ab	41.81±1.78b	48.16±1.30a	44.37±1.68ab
Vigour Index	4079.17±76.40b	3696.67±44.10c	4392.59±50.17a	3975.00±28.79b
Water content (%)	94.33±0.13ab	94.77±0.35a	93.13±0.38b	93.70±0.35ab
RWC (%)	89.73±1.04b	94.36±1.80a	84.67±0.52c	88.00±1.76bc
H$_2$O$_2$ (µmol g^{-1}DW)	70.06±2.42b	91.43±1.49a	38.95±1.51d	49.21±2.55c
TBARS (nmol g^{-1}DW)	259.34±19.15b	388.38±7.91a	247.54±25.31b	278.83±5.28b
Proline (µmol g^{-1}DW)	78.64±2.14a	53.29±1.54b	44.19±1.63c	38.63±3.67c
Total ascorbate (µmol g^{-1}DW)	108.68±1.08b	128.23±3.01a	97.54±1.33c	106.90±0.37b
ASA/DHA	1.10±0.03c	0.97±0.05c	1.60±0.05b	1.79±0.04a
Total glutathione (µmol g^{-1}DW)	1.22±0.06b	1.43±0.05a	0.97±0.06c	1.09±0.02bc
GSH/GSSG	2.53±0.27b	1.71±0.13b	5.81±0.74a	2.01±0.13b
APX (U g^{-1} protein)	606.60±7.40a	510.27±18.17b	500.63±7.92b	510.80±20.51b
GPX (U g^{-1} protein)	1196.67±11.87a	1037.30±8.45a	1032.57±34.03a	1022.02±67.67a
POD (U g^{-1} protein)	1522.02±38.60c	1647.61±34.12b	1415.27±16.42d	2239.91±20.73a
CAT (U g^{-1} protein)	5049.53±487.63a	3832.88±387.16b	2649.43±131.83b	3031.52±282.09b

709
710 Data are the mean of at least three replicates ± SE. Means followed by the same letters within the same row are not
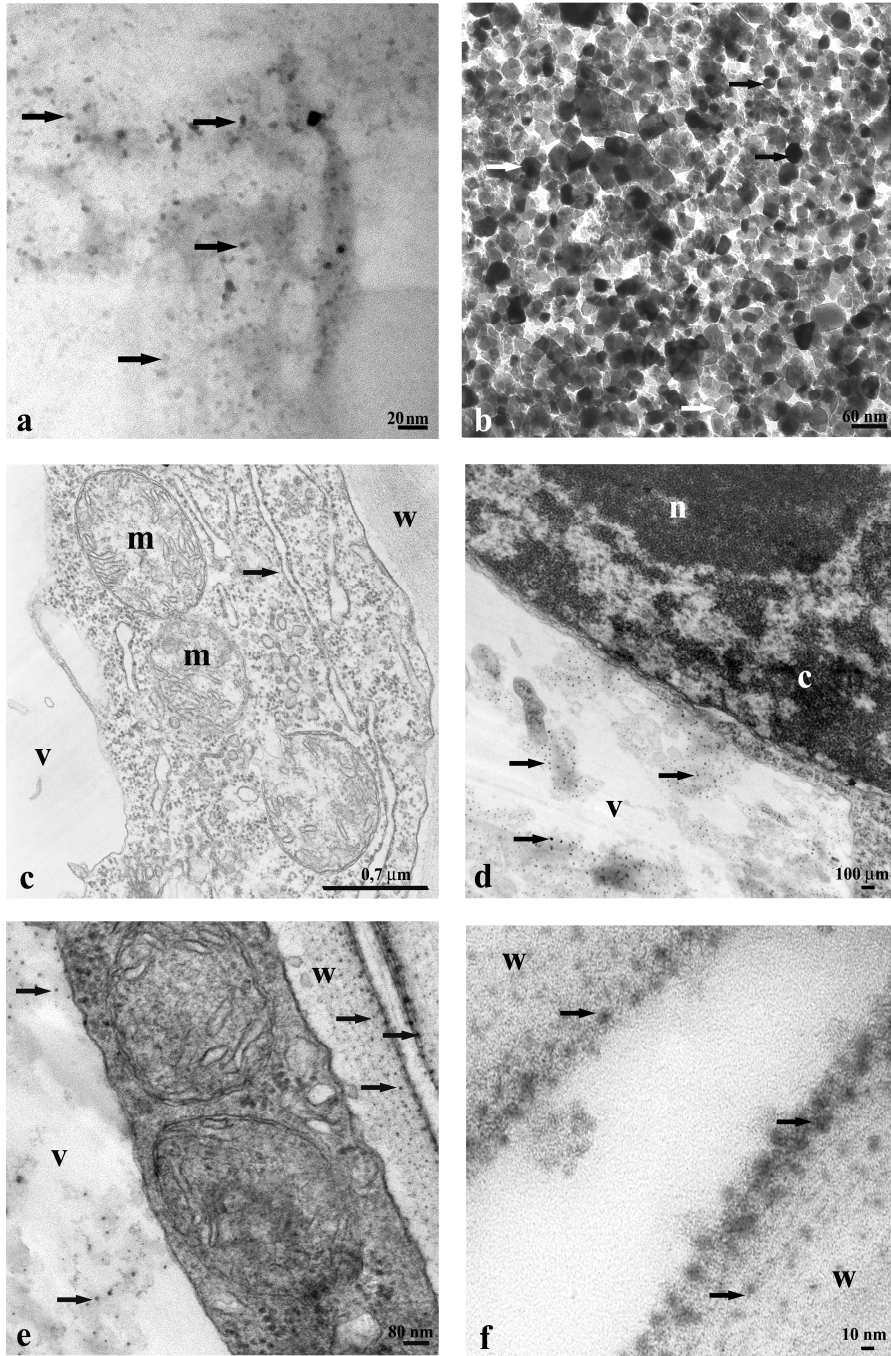711 significantly different at 1%.
712

Control   P-NPs   S-NPs   Bulk
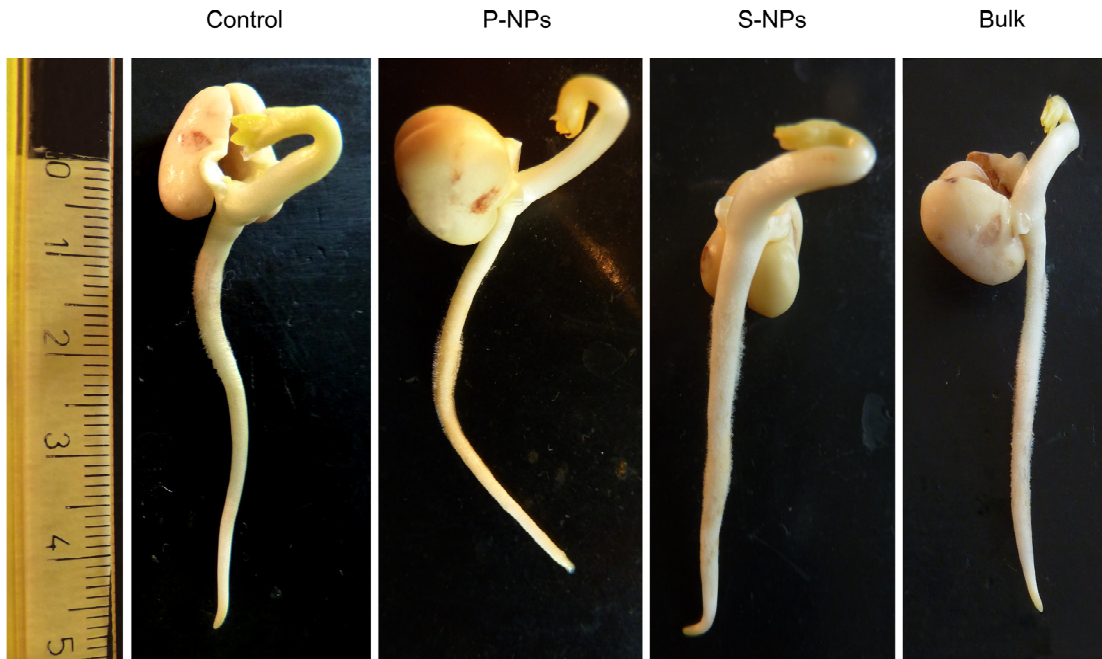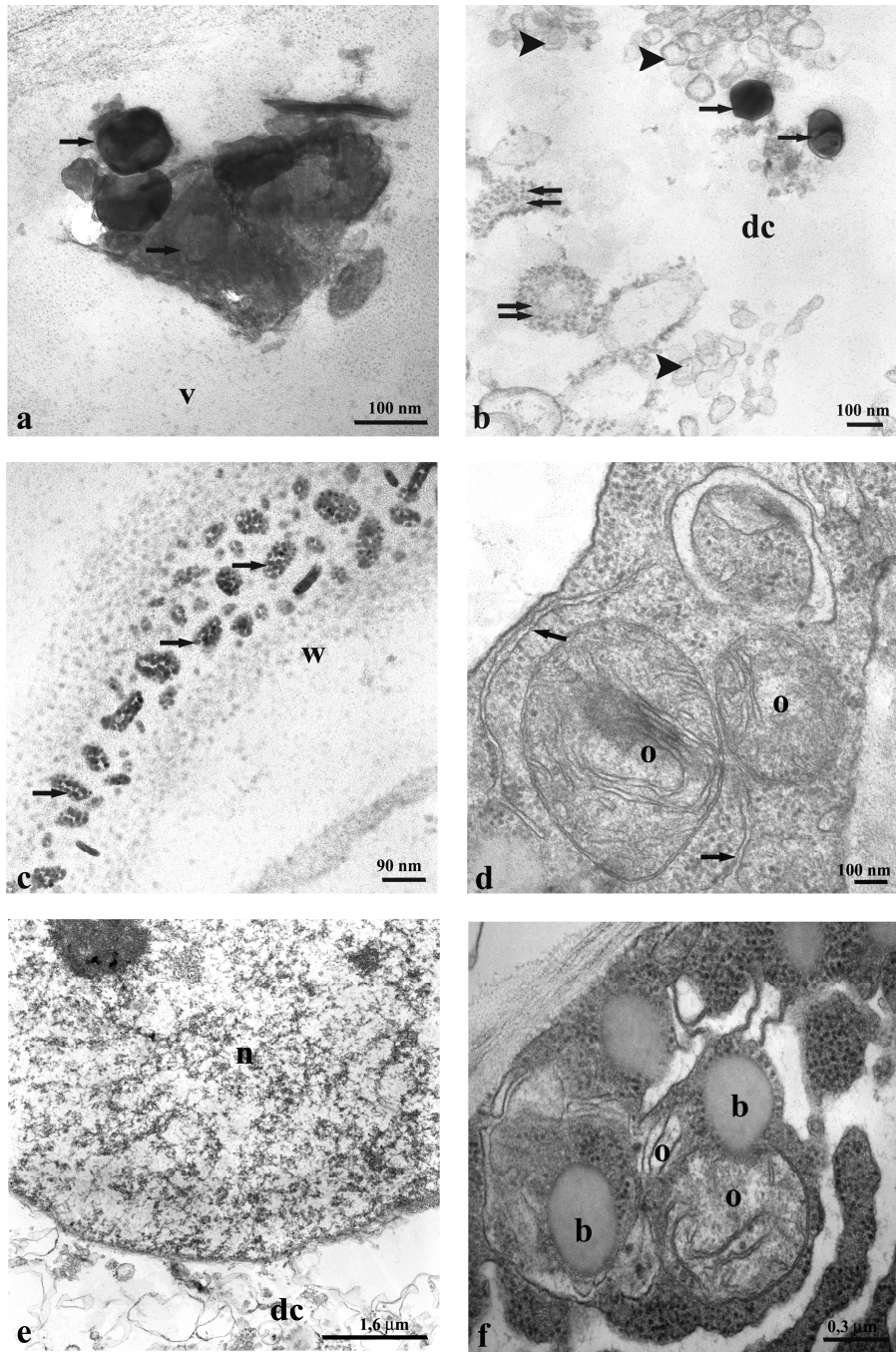
713

714 Figure 1

715

716

717

718

719
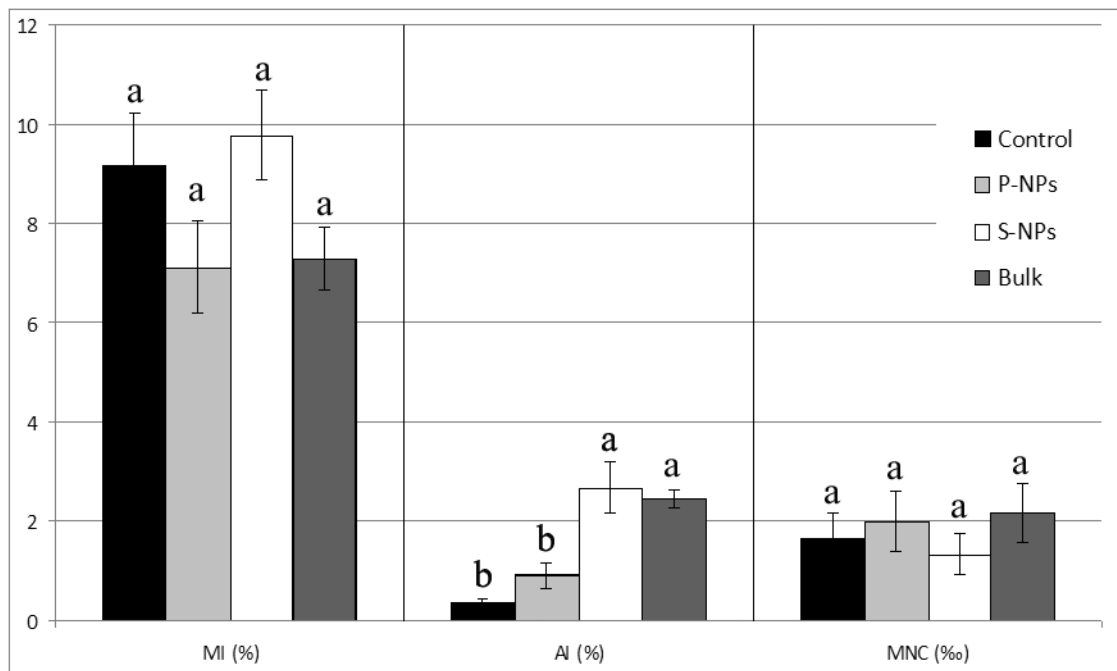720   Figure 2
721
722

724   Figure 3

727

728

729

730

731 Figure 4

732

733

734

735

736

737

738

739

740

741

742

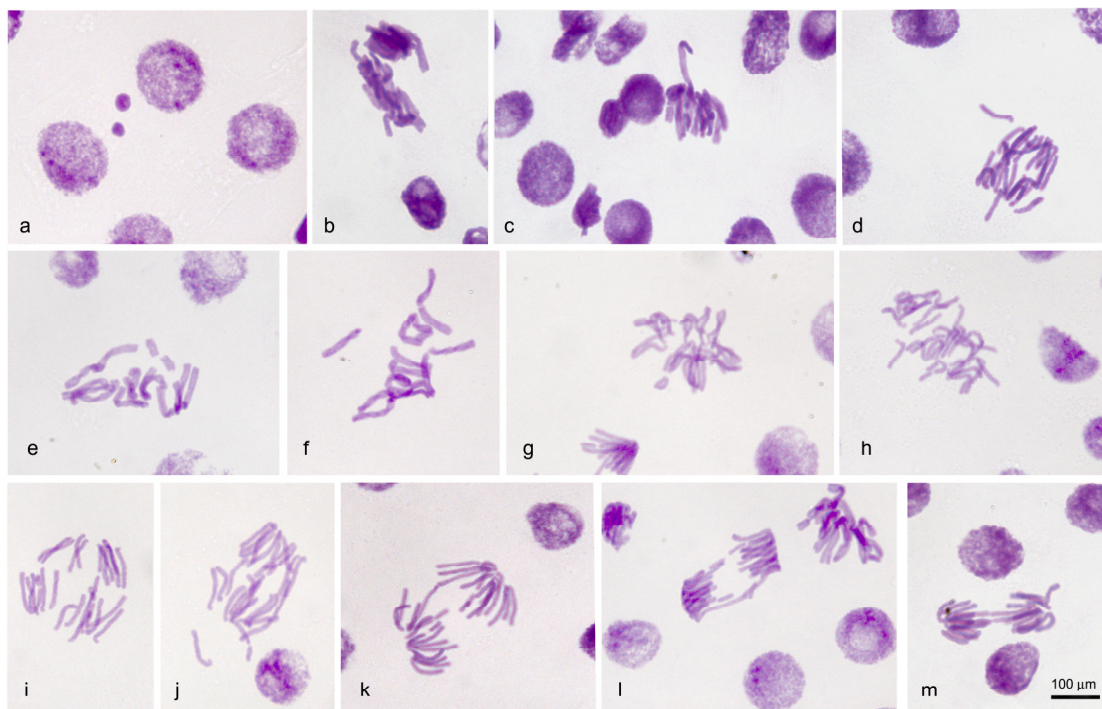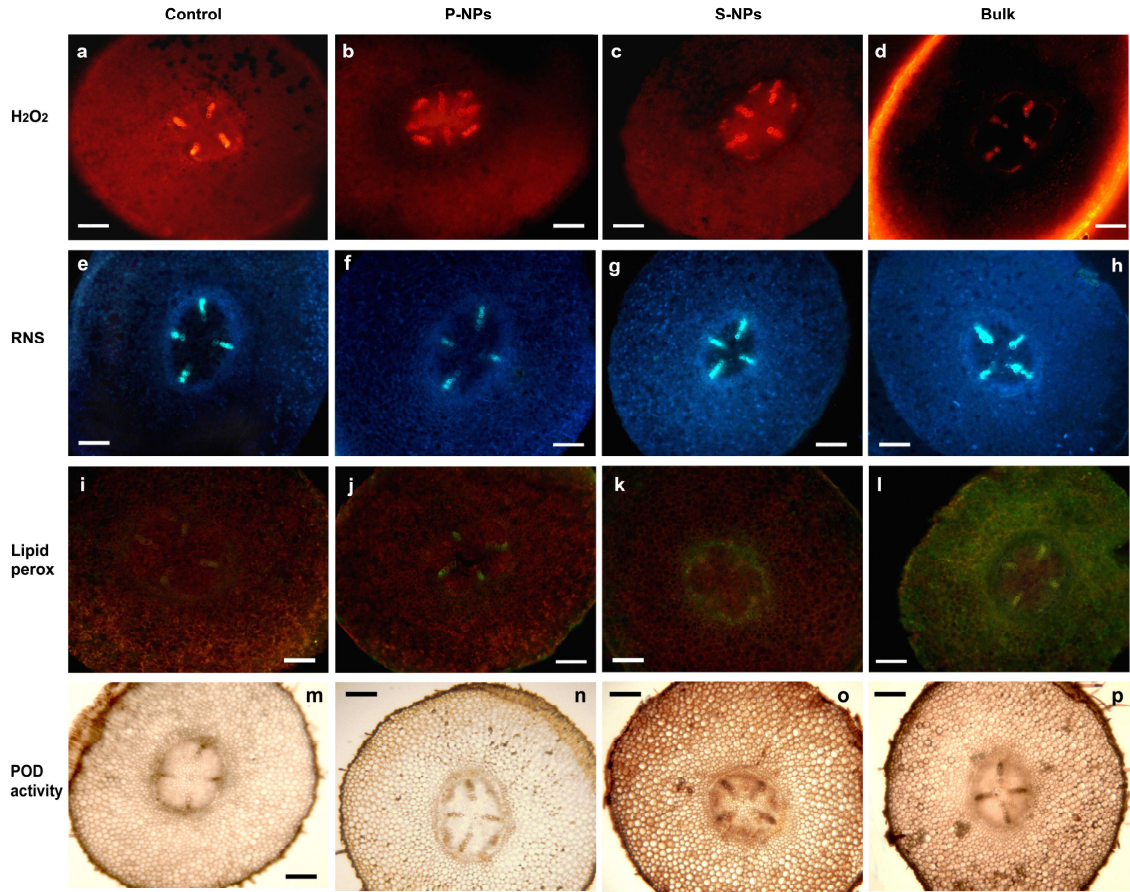743

744

745

746

747

Figure 5

768

769   Figure 6

770

771

772

773

774

775

776

777

778

779

780

781

782

783

784

785

786

787

788

789

790

791

792

793

794

795

796

797